IEEE Access
Multidisciplinary | Rapid Review | Open Access Journal

Received December 27, 2021, accepted January 4, 2022, date of publication January 7, 2022, date of current version January 13, 2022.

Digital Object Identifier 10.1109/ACCESS.2022.3141543

Geometric Sequence Decomposition-Based Interference Cancellation in Automotive Radar Systems

WOONG-HEE LEE[1], (Member, IEEE), AND SEONGWOOK LEE[2], (Member, IEEE)
[1]Department of Control and Instrumentation Engineering, Korea University, Sejong-si 30019, Republic of Korea
[2]School of Electronics and Information Engineering, College of Engineering, Korea Aerospace University, Gyeonggi-do 10540, Republic of Korea

Corresponding author: Seongwook Lee (swl90@kau.ac.kr)

This work was supported in part by the Institute of Information & Communications Technology Planning & Evaluation (IITP) funded by the Korean Government [Ministry of Science and ICT (MSIT)] under Grant 2021-0-00237, and in part by the National Research Foundation of Korea (NRF) funded by the Korean Government (MSIT) under Grant 2021R1G1A1094195.

ABSTRACT Radar signals generated from other vehicles can act as interference to ego-vehicle, which degrades the inherent detection performance of radar. In this paper, we address an efficient solution to the interference problem in frequency-modulated continuous wave (FMCW)-based automotive radar systems, named geometric sequence decomposition based interference cancellation (GSD-IC). With the method of GSD-IC, we can decompose the received signal into different non-orthogonal superposed signals, which means the interference signal and the signal reflected from the desired target are separated. It is based on the facts that 1) each single sampled signal can be interpreted as a geometric sequence and 2) the useful physical features, such as the time delay and the Doppler frequency, are extracted after converting the superposition of these geometric sequences into several transformed matrices. Through this approach, we can achieve effective interference signal cancellation while minimizing the loss of meaningful target information. Moreover, the proposed method does not require the generation of specific radar waveforms, and can mitigate interference through signal processing even with existing waveforms. Numerical results show that our algorithm outperforms existing methods in various scenarios.

INDEX TERMS Automotive frequency-modulated continuous wave (FMCW) radar, geometric sequence decomposition (GSD), interference cancellation, joint delay and Doppler estimation.

I. INTRODUCTION

In recent years, automotive sensors for autonomous driving, such as radar, lidar, camera, and ultrasonic sensors, are getting attention. These sensors are mounted on the automobiles to provide safety and convenience for the driver. Among these sensors, the importance of the radar sensor has been emphasized because of its robustness to the weather conditions and longer detection range than other automotive sensors [1]. As an automotive radar, frequency-modulated continuous wave (FMCW) radars operating in the 77-81 GHz are widely used due to the low power consumption and high range resolution [2]. This automotive FMCW radar can be used to estimate the exact location of the target, classify the types of detected targets [3], [4] and recognize road environments [5], [6].

As the number of vehicles equipped with automotive radar systems increases, interference between automotive radar systems will inevitably occur [7]. When an FMCW radar signal transmitted from another vehicle is received by the radar of ego-vehicle, the signal acts as an interference. If the frequency difference between the transmitted signal of the ego-vehicle and the interference signal is smaller than the cut-off frequency of the low-pass filter, a signal with undesired frequency components is detected [8]. In addition, the intensity of the interference signal is 30 dB higher than that of the signal reflected from the desired target [9]. Thus, the beat frequency corresponding to the desired target is buried by interference, and the desired target may not be detected [10]. Because missing the target can be a great risk to the driver using automotive radar functions, such as

The associate editor coordinating the review of this manuscript and approving it for publication was Mauro Gaggero.

adaptive cruise control and autonomous emergency braking, an efficient method to suppress the effects of interference has to be devised.

Several studies have been conducted to mitigate the effect of interference between automotive FMCW radar systems. In [11]–[16], the authors devised new waveforms or modified existing waveforms to avoid the interference. For example, the pseudo-noise coded FMCW radar signals [11], [12] and the orthogonal noise waveform [13] were proposed. In addition, the frequency hopping was used with the FMCW radar system [14] or a method of irregularly changing the sweep time and the bandwidth of the FMCW radar signal was also presented in [15], [16]. Moreover, research to suppress the interference through signal processing techniques has been proposed [9], [17]–[21] without changing the existing radar hardware. In [9], the author eliminated the interference by padding zeros in the interval where the interference occurred. When the interference interval is short, interference can be effectively suppressed without loss of the desired target information even by the method proposed in [9]. However, if the interval is long, the information of the target may be erased by the zero-padding. To overcome such a problem, the authors reconstructed the interference signal by estimating its amplitude and phase and suppressed the interference by subtracting it from the original received signal [17], [18]. In addition, the authors in [19] presented the signal processing technique that can effectively suppress the mutual interference in the time-domain received signal. Recently, a wavelet transform-based interference cancellation technique has been introduced in [20], and a method of mitigating interference in transform domains where the desired signal and the interference are effectively separated has been proposed in [21].

In this paper, as a new approach, we propose a method to extract the interference signal itself from the received signal. The radar signals received by the ego-vehicle includes signals reflected from the desired target and the interferer, and even a signal transmitted from the interferer. Those signals have different characteristics in the complex gain, time delay, and the Doppler shift. To deal with these problems, we propose an entirely different approach to the cancellation of interference signal. First of all, we explore the potential of the geometric sequential representation in time and frequency domains to pinpoint the desired and interference signals in the FMCW radar systems. Next, we exploit the fact that the non-orthogonally overlapped K baseband signals, i.e., the mixture of desired and interference signals, constitute a superposition of K geometric sequences. This mathematical property converts the joint delay and Doppler estimation problem in the FMCW radar systems into the extraction of the parameters of geometric sequences from the two-dimensional (2D) data samples.

The most notable property of geometric sequence decomposition based interference cancellation (GSD-IC) is that it results in the high resolution for joint delay and Doppler estimation. This is because the proposed scheme directly extracts the intrinsic information of the received signal. Acquiring the parameters in GSD-IC is equivalent to solving an K-th order polynomial equation. Overall, GSD-IC significantly reduces the joint delay and Doppler estimation error compared to the conventional methods such as fast Fourier transform (FFT), which is manly based on linear correlation. Unlike the methods changing the radar waveforms in [11]–[16], we can mitigate the interference by simple signal processing without changing the existing radar hardware. In addition, because the proposed interference coordination extracts the desired target signal and the interference signal from the actual received radar signal, it is different from the methods [17], [18] of mathematically modeling the interference signal. Moreover, compared to the suppression method in [19], it is not necessary to set or adjust the parameter values according to each FMCW radar system in our proposed method.

The remainder of the paper is organized as follows. First, in Section II, we introduce the interference signal model in the FMCW automotive radar systems. Then, the concept and basic principles of joint estimation of delay and Doppler are introduced in Section III. In addition, the proposed GSD-IC method that separates the interference signal and desired target signals is presented in this section. Next, the performance of the proposed method is verified through simulations in Section IV. Finally, we conclude this paper in Section V.

The following symbols will be used throughout the paper:

- $K \in \mathbb{N}$: the number of signals.
- $\mathbf{s}_k \in \mathbb{C}^{N\times M}$: the k-th baseband signal.
- $\mathbf{w} \in \mathbb{C}^{N\times M}$: additive noise.
- $\mathbf{s} := \sum_{k=1}^{K} \mathbf{s}_k + \mathbf{w}$: summation of $\mathbf{s}_k$ with noise, i.e., the entire received signal.
- $\mathbf{s}_{n,:} \in \mathbb{C}^{1\times M}$: the n-th row of $\mathbf{s}$, where $n \in \{0, \cdots, N-1\}$.
- $\mathbf{s}_{:,m} \in \mathbb{C}^{N\times 1}$: the m-th column of $\mathbf{s}$, where $m \in \{0, \cdots, M-1\}$.
- $\alpha_k \in \mathbb{C}$: complex-valued amplitude of $\mathbf{s}_k$.
- $T_{d,k} \in \mathbb{R}$: time delay of the k-th signal.
- $f_{D,k} \in \mathbb{R}$: Doppler frequency of the k-th signal.
- $R_1 \in \mathbb{R}$: relative distance between the ego-vehicle and the target.
- $V_1 \in \mathbb{R}$: relative velocity between the ego-vehicle and the target.
- $\hat{R}_1 \in \mathbb{R}$: estimate of R_1.
- $\hat{V}_1 \in \mathbb{R}$: estimate of V_1.
- c: speed of light.
- f_c: center frequency of the FMCW radar.
- S: time-frequency slope of the FMCW radar.
- T_{SW}: sweep time of the FMCW radar.
- f_s: sampling frequency at the ego-vehicle.
- $\mathcal{R}_K$: function of extracting of K common ratios to estimate delay and Doppler information.
- $\mathcal{D}_K$: function of denoising the noisy input sequence.

II. SIGNAL MODEL IN FMCW RADAR SYSTEMS

Transmitting multiple bundles of signals whose frequency increases linearly over a short period of time is most effective

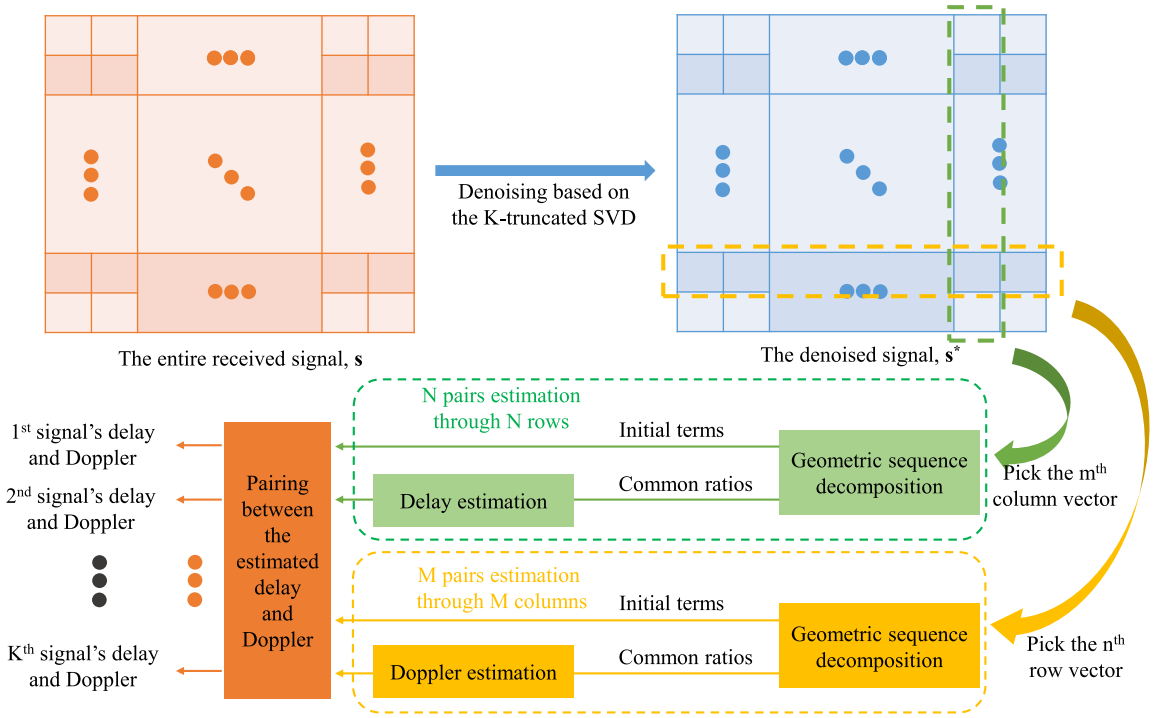

FIGURE 1. An illustration of the joint time and Doppler estimation based on geometric sequence decomposition.

for distance and velocity estimation among various FMCW radar systems [22]. In this radar systems,[1] $\mathbf{s}(n, m)$ can be expressed as

$$\begin{aligned}\mathbf{s}(n,m) &= \sum_{k=1}^{K} \mathbf{s}_k(n,m) + \mathbf{w}(n,m) \\ &= \sum_{k=1}^{K} \alpha_k \exp\{j2\pi[(T_{d,k}S + f_{D,k})\frac{n}{f_s} \\ &\quad + f_{D,k}T_{SW}m + f_c T_{d,k}]\} + \mathbf{w}(n,m), \end{aligned} \tag{1}$$

for all n, m. Here, the Doppler frequency is very small compared to the distance-related frequency, i.e., $T_{d,k}S \gg f_{D,k}$. Thus, $\mathbf{s}_k(n, m)$ in (1) can be simplified as

$$\begin{aligned}\mathbf{s}(n,m) = \sum_{k=1}^{K} \alpha_k \exp\{j2\pi(&\frac{T_{d,k}S}{f_s}n \\ &+ f_{D,k}T_{SW}m + f_c T_{d,k})\} + \mathbf{w}(n,m), \end{aligned} \tag{2}$$

for all n, m. Generally in fast-ramp FMCW radar systems, the received signal in (2) can be regarded as two-dimensional data sampled at a sampling frequency of f_s on the slow time axis and $\frac{1}{T_{SW}}$ on a fast time axis. Thus, if a 2D FFT is applied to the baseband signal in (2), one can extract the delay and Doppler information of the signal from the peak point correspond to $(T_{d,k}, f_{D,k})$ for all k [22]. This FFT-based joint delay and Doppler estimation has been conventionally used in radar systems. To guarantee the performance of the FFT-based estimation method, a given radar signal must be sufficiently sampled at wide intervals. If the number of sampled points is insufficient, the estimation capability of the method is rapidly degraded. Therefore, there is a need for an efficient estimation method capable of having a higher resolution while supplementing the limitations of the FFT-based estimation method.

[1]For simplicity, we assume a single antenna radar system.

III. METHODOLOGY OF GSD-IC

The objective of the FMCW radar is to obtain the accurate delay and Doppler through the received signal. For this, it should be possible to derive values that are as close to $\{T_{d,k}, f_{D,k}\}_{k=1}^{K}$ as possible by processing two dimensional data $\mathbf{s}$. The following subsections will describe a new high resolution technique for estimating $\{T_{d,k}, f_{D,k}\}_{k=1}^{K}$ based on the mathematical characteristic of $\mathbf{s}$, which is the geometric sequential representation. The overall concept of joint delay and Doppler estimation is depicted in Fig. 1.

A. GEOMETRIC SEQUENTIAL REPRESENTATION IN 2D SAMPLES

Before describing GSD-IC, let us look at the interesting mathematical properties of $\mathbf{s}$ toward the geometric sequential representation. For this, let us have a close look at the property of the arbitrary row and column in $\mathbf{s}_k \in \mathbb{C}^{N\times M}$. Recalling (2), let $\mathbf{s}_{k,n,:} \in \mathbb{C}^{1\times M}$ and $\mathbf{s}_{k,:,m} \in \mathbb{C}^{N\times 1}$ be the n-th row and the m-th column of $\mathbf{s}_k$, respectively. Then, $\mathbf{s}_{k,n,:}$ can be represented as follows:

$$\alpha_k e^{j2\pi(\frac{T_{d,k}S}{f_s}n + f_c T_{d,k})}\{1, e^{j2\pi f_{D,k}T_{SW}}, e^{j2\pi 2f_{D,k}T_{SW}}, \cdots\}. \tag{3}$$

One can notice that (3) is a geometric sequence with the initial term of $\alpha_k e^{j2\pi(\frac{T_{d,k}S}{f_s}n+f_cT_{d,k})}$ and the common ratio of $e^{j2\pi f_{D,k}T_{SW}}$. This means that $\mathbf{s}_{n,:}$ can be regarded as a non-orthogonal superposition of K number of geometric sequences. As we know, a geometric sequence is characterized by two parameters: initial term and common ratio. Let $\mathbf{a}_{n,:}, \mathbf{r}_{n,:} \in \mathbb{C}^K$ be the vectors of initial terms and common ratios of the geometric sequences consisting of $\mathbf{s}(n, :)$. In other words,

$$\begin{aligned}\mathbf{a}_{n,:} &= [\alpha_k e^{j2\pi(\frac{T_{d,1}S}{f_s}n+f_cT_{d,1})}, \cdots, \alpha_K e^{j2\pi(\frac{T_{d,K}S}{f_s}n+f_cT_{d,K})}],\\ \mathbf{r}_{n,:} &= [e^{j2\pi f_{d,1}T_{SW}}, \cdots, e^{j2\pi f_{D,K}T_{SW}}].\end{aligned} \tag{4}$$

Similarly, $\mathbf{s}_{k,:,m}$ can be also represented as follows:

$$\alpha_k e^{j2\pi(f_{D,k}T_{SW}m+f_cT_{d,k})}\{1, e^{j2\pi\frac{T_{d,k}S}{f_s}}, e^{j2\pi\frac{2T_{d,k}S}{f_s}}, \cdots\}. \tag{5}$$

Thus,

$$\begin{aligned}\mathbf{a}_{:,m} &= [\alpha_1 e^{j2\pi(f_{d,1}T_{SW}m+\frac{f_cR_1}{c})}, \cdots, \alpha_K e^{j2\pi(f_{D,k}T_{SW}m+\frac{f_cR_K}{c})}],\\ \mathbf{r}_{:,m} &= [e^{j2\pi\frac{T_{d,1}S}{f_s}}, \cdots, e^{j2\pi\frac{T_{d,K}S}{f_s}}].\end{aligned} \tag{6}$$

B. JOINT DELAY AND DOPPLER ESTIMATION IN IDEAL CASE

In this section, we assume the ideal case which means that $\mathbf{w}(n, m) = 0$ for any n and m. As mentioned in Section III-A, the received signal in (2) can be recognized as the sum of geometric sequences. Thus, to decompose the interference signal and the desired signal from the received signal, we employ the method of geometric sequence decomposition with K-simplexes transform (GSD-ST). The GSD-ST is a mathematical technique for decomposing the summed geometric sequences, which was proposed in [23]. The fundamental idea of GSD-ST is to transform an observed sequence to multiple K-simplexes in a virtual K-dimensional space and to correlate the volumes of the transformed simplexes. Through the proper transformation of the observed sequence, the method requires only $2K + 1$ samples of the superposed sequence to completely decompose it as K individual sequences. In addition, the required samples further reduce to $2K$ if K is known a priori. Thus, the proposed GSD-IC scheme builds on the method of GSD-ST based on the fact that $\mathbf{s}_{n,:}$ and $\mathbf{s}_{:,m}$ are represented as the superposition of K number of geometric sequences for all n and m. For simplicity, we assume that K is known *a priori*. Consequently, we will utilize the fact that any row and column of the two-dimensional FMCW signal, $\mathbf{s}$, is modeled with K geometric sequences.

1) DOPPLER ESTIMATION

To estimate the Doppler frequencies of signals, we will obtain $\mathbf{a}_{n,:}$ and $\mathbf{r}_{n,:}$ with the information of known K, based on an arbitrary row vector $\mathbf{s}_{n,:}$. According to [23], we define a l-th vertex in the K-dimensional space, $\mathbf{v}_l \in \mathbb{C}^K$, as follows:

$$\mathbf{v}_l = [\mathbf{s}_{n,:}(l), \cdots, \mathbf{s}_{n,:}(l + K - 1)]^T. \tag{7}$$

Let us construct $K + 1$ number of consecutive vertices, $\mathbf{v}_0, \cdots, \mathbf{v}_K$ as (7). Next, let $\aleph$ be a series of K-simplexes whose length is $K + 1$, which is formed by lexicographically combinatorial order as follows:

$$\aleph = \{(\chi_K(\mathbf{v}_0, \cdots, \mathbf{v}_{K-1})), \cdots, (\chi_K(\mathbf{v}_1, \cdots, \mathbf{v}_K))\}. \tag{8}$$

According to Theorem 2 in [23], $\mathbf{r}_{n,:}$ is equal to the roots of the following K-th order polynomial equation:

$$\sum_{l=0}^{K} \Lambda(\aleph[l])(-r)^{L-l} = 0. \tag{9}$$

Thus, the function extracting the common ratios, $\mathcal{R}_K$, is equivalent to the process of (7), (8), and (9), where P is the length of the input sequence. This means that

$$\mathbf{r}_{n,:} = \mathcal{R}_K(\mathbf{s}_{n,:}). \tag{10}$$

Once $\mathbf{r}_{n,:}$ is obtained, $\mathbf{a}_{n,:}$ can be simply found by the following matrix pseudo-inversion:

$$\mathbf{a}_{n,:} = \mathbf{R}^+_{n,:}\mathbf{s}_{n,:}, \tag{11}$$

where $\mathbf{R}_{n,:} \in \mathbb{C}^{K\times M}$ is the matrix constructed by $\mathbf{r}_{n,:}$ satisfying $\mathbf{R}_{n,:}[i, j] := (\mathbf{r}_{n,:}[i])^j$ for $i, j = 0, 1, 2, \cdots$, and $(\cdot)^+$ is the pseudo-inverse operation.

The extraction of the parameters $f_{D,k}$, i.e., Doppler estimation, is straightforward from $\mathbf{r}_{n,:}$, and the predetermined value of T_{SW}. Denote $\hat{f}_{D,k}$ is the estimate of $f_{D,k}$, then it can be represented as follows for all k:

$$\hat{f}_{D,k} = \frac{\angle\mathbf{r}_{n,:}(k)}{2\pi T_{SW}}, \tag{12}$$

where $\angle(\cdot)$ is the phase of an complex-valued input.

2) DELAY ESTIMATION

Recalling (5) and (6), we can obtain $\mathbf{r}_{:,m}$ as follows for all m:

$$\mathbf{r}_{:,m} = \mathcal{R}_K(\mathbf{s}_{:,m}). \tag{13}$$

Thus, delay information can be also found with the predetermined value of S as follows for all k':

$$\hat{T}_{d,k'} = \frac{f_s\angle\mathbf{r}_{:,m}(k')}{2\pi S}. \tag{14}$$

3) PARING BETWEEN ESTIMATED VALUES OF DELAY AND DOPPLER

We show that the processes of obtaining $\{\hat{f}_{D,k}\}_{k=1}^K$ and $\{\hat{T}_{d,k'}\}_{k'=1}^K$. However, there is no information about which $\hat{f}_{D,k}$ is mapped to which $\hat{T}_{d,k'}$. Therefore, we will explain how to pair between $\{\hat{f}_{D,k}\}_{k=1}^K$ and $\{\hat{T}_{d,k'}\}_{k'=1}^K$, i.e., how to identify $\{T_{d,k}, f_{D,k}\}_{k=1}^K$ from $\{\hat{f}_{D,k}\}_{k=1}^K$ and $\{\hat{T}_{d,k'}\}_{k'=1}^K$ in this subsection.

First, let us look at two consecutive rows in $\mathbf{s}$, i.e., $\mathbf{s}_{n,:}$ and $\mathbf{s}_{n+1,:}$. From these, we can extract $\{\mathbf{a}_{n,:}, \mathbf{r}_{n,:}\}$ and $\{\mathbf{a}_{n+1,:}, \mathbf{r}_{n+1,:}\}$ based on (9) and (11). Here, $\mathbf{r}_{n,:}$ and $\mathbf{r}_{n+1,:}$ are identical based on (4), which are the sources to obtain $\{\hat{V}_k\}_{k=1}^K$, as we mentioned in Section III-B1. However, we can find an interesting property from $\mathbf{a}_{n,:}$ and $\mathbf{a}_{n+1,:}$.

Recalling (4), we can observe that

$$\mathbf{a}_{n,:}(k) = \alpha_k e^{j2\pi(\frac{T_{d,k}S}{f_s}n+\frac{f_c R_k}{c})},$$
$$\mathbf{a}_{n+1,:}(k) = \alpha_k e^{j2\pi(\frac{T_{d,k}S}{f_s}(n+1)+\frac{f_c R_k}{c})}, \tag{15}$$

for all n, k. Based on this progression from $\mathbf{a}_{n,:}(k)$ to $\mathbf{a}_{n+1,:}(k)$, we can extract new estimate of $\hat{T}_{d,k}$, which can be denoted by $\hat{T}'_{d,k}$. More generally, if we define $\mathbf{a}_{:}^{(k)}$ as $\{\mathbf{a}_{n,:}(k)\}_{n=0}^{N-1}$, then $\hat{R}'_k$ is obtained in the single common ratio of $\mathbf{a}_{:}^{(k)}$ for all k. Thus, $\hat{T}'_{d,k}$ can be extracted as follows:

$$\hat{T}'_{d,k} = \frac{f_s \angle(\mathcal{R}_1(\mathbf{a}_{:}^{(k)}))}{2\pi S}. \tag{16}$$

Finally, we can construct the rule of pairing as follows:

$$k = \{k' | \hat{T}_{d,k'} = \hat{T}'_{d,k}\}, \tag{17}$$

for all k. It is obvious that (17) can be applied in vice versa, i.e., by executing the above processes starting from the consecutive columns in $\mathbf{s}$.

4) COMPLEXITY ANALYSIS

The computational complexity of GSD-IC is $\mathcal{O}((K+1)K^{2.373})$, which is equivalent to obtaining $\{\det \aleph[j]\}_{j=0}^{K}$ if $K \leq 4$. Otherwise, eigenvalue decomposition of K-by-K companion matrix is additionally required, i.e., eventually $\mathcal{O}((K+2)K^{2.373})$ [24]. This is because the major computation of GSD-SCE is devoted to constructing and solving (9), i.e., the K-th order polynomial equation. Therefore, it is extremely efficient when $K \leq 4$. It is noteworthy that the complexity of GSD-IC is free from the dimension of the observed signal, only dependent on K. This is a clear difference from the conventional methods, which are inevitably dependent on the dimension of observations.

C. DENOISING PROCESS IN NOISY CASE

We will introduce the methods of denoising and error suppression as a pre- and post-process, respectively, of delay and Doppler estimation. In the previous section, we have assumed that the observation of $\mathbf{s}$ is flawless. However, the observed 2D data may be prone to noise particularly in automotive radar systems. Thus, we present the practical ways of mitigating errors in $\mathbf{s}$ in this section. To model this, we assume that $w(n, m)$ follows the complex Gaussian distribution for any n and m.

1) VECTOR-WISE DENOISING: ITERATIVE TRUNCATED SVD

The fundamental approach of the de-noising process is to utilize more samples than the minimum requirement, i.e., to consider $N, M > 2K$.

First, let us focus a row vector of $\mathbf{s}$, i.e., $\mathbf{s}_{n,:}$. Here, $\mathbf{s}_{n,:}$ is an index-wise correlated sequence with $2K$ parameters, i.e., K-pairs of initial term and common ratio, of interest, whereas $w_{n,:}$ is a sequence of random variables. We focus on the fact that $\mathbf{s}$ has K number of non-identical bases. Further, each basis is made by only one parameter, i.e., the common ratio, from the nature of the geometric sequence. From this perspective, the de-noising of $\mathbf{s}_{n,:}$ can be handled by suppressing the number of bases for $\mathbf{s}_{n,:}$ to K. Thus, we utilize the iterative K-truncated singular value decomposition (SVD) for only taking the K largest singular values and their corresponding vectors.

From this, the denoising function $\mathcal{D}_K(\cdot)$ can be the following process (where $\mathbf{b}_w \in \mathbb{C}^P$ is an arbitrary sequence.):

i) Make a matrix, $\mathbf{Q} \in \mathbb{C}^{P_h \times (P-P_h+1)}$ where $P_h = \lfloor \frac{P+1}{2} \rfloor$ from $\mathbf{b}_w$ satisfying the condition:
$$\mathbf{Q}(i, j) := \mathbf{b}_w(i+j), \tag{18}$$
where $i, j \in \{0, 1, \cdots\}$.
ii) Execute the K-truncated SVD of $\mathbf{Q}$.
iii) Reconstruct $\mathbf{Q}$ using the K-tuples of singular values and vectors.
iv) Transform $\mathbf{Q}$ onto a new $\mathbf{b}_w$ by averaging the values with the same index, i.e.
$$\{\mathbf{b}_w(l)\}_{l=0}^{P-1} := \frac{1}{q}\sum_{n,m}\mathbf{Q}(m, n), \quad \text{s.t. } m+n=l, \tag{19}$$
where $q = l+1$ if $l < P_h$, and $q = P-l$ otherwise.
v) Repeat the above four-step process with the stopping criterion ϵ until $\mathbf{b}_w$ converges to the fixed sequence denoted by $\mathbf{b}_w^*$.

The process of $\mathcal{D}_K(\cdot)$ is equivalent to making the bases of $\mathbf{Q}$ for both row space and column space identical to each other, aiming to minimize the number of parameters in $\mathbf{b}_w$. Using this denoising function $\mathcal{D}_K(\cdot)$, we can obtain the denoised sequences, $\mathbf{s}_{n,:}^*$ and $\mathbf{s}_{:,m}^*$, as follows:

$$\mathbf{s}_{n,:}^* = \mathcal{D}_K(\mathbf{s}_{n,:}) \quad \text{and } \mathbf{s}_{:,m}^* = \mathcal{D}_K(\mathbf{s}_{:,m}), \tag{20}$$

for all n, m.

2) PARAMETER-WISE ERROR SUPPRESSION AND PAIRING

Let $\{\hat{T}_{d,k'}^{(m)}\}_{k'=1}^{K}$ denotes the output of (14) after obtaining $\mathbf{r}_{:,m}(k')$ from $\mathcal{R}_K(\mathbf{s}_{:,m}^*)$ for all m. Naturally, we can obtain the final form of the estimated delay as follows:

$$\hat{T}_{d,k'} = \frac{1}{M}\sum_{m=0}^{M-1}\hat{T}_{d,k'}^{(m)}, \tag{21}$$

for all k'.

In addition, let $\{\hat{f}_{D,k}^{(n)}\}_{k=1}^{K}$ denotes the output of (12) after obtaining $\mathbf{r}_{n,:}(k)$ from $\mathcal{R}_K(\mathbf{s}_{n,:}^*)$ for all n. Here, we can also obtain the final form of the estimated Doppler frequency as follows:

$$\hat{f}_{D,k} = \frac{1}{N}\sum_{n=0}^{N-1}\hat{f}_{D,k}^{(n)}, \tag{22}$$

for all k.

For the pairing between the estimated delay and Doppler, (16) can be reformulated as follows due to the noisy samples:

$$\hat{T}'_{d,k} = \frac{f_s \angle(\mathcal{R}_1(\mathcal{D}_1(\mathbf{a}_{:}^{(k)})))}{2\pi S}. \tag{23}$$

Here, (17) is also reformulated as follows:

$$k = \arg\min_{k'} |\hat{T}_{d,k'} - \hat{T}'_{d,k}|, \tag{24}$$

for all k, k'. Again, it is obvious that this process can be applied vice versa. Algorithm 1 depicts the procedure of obtaining $\{\hat{f}_{D,k}, \hat{T}_{d,k}\}_{k=1}^{K}$ from $\mathbf{s}$.

Algorithm 1 Procedure of Obtaining $\{\hat{f}_{D,k}, \hat{T}_{d,k}\}_{k=1}^{K}$

i) Set the 2-D observed sequence, $\mathbf{s} := \sum_{k=1}^{K} \mathbf{s}_k + \mathbf{w}$.
[*Phase 1*: Denoising $\mathbf{s}$]
ii) Denoise $\mathbf{s}_{n,:}$ and $\mathbf{s}_{:,m}$ as $\mathbf{s}^*_{n,:}$ and $\mathbf{s}^*_{:,m}$, respectively, based on (20) for all n, m.
[*Phase 2*: Estimating K pairs of Doppler and delay]
iii) Obtain $\{\hat{f}_{D,k}\}_{k=1}^{K}$ based on (10), (12), and (22).
iv) Obtain $\{\hat{T}_{d,k'}\}_{k'=1}^{K}$ based on (13), (14), and (21).
[*Phase 3*: Paring between $\{\hat{f}_{D,k}\}_{k=1}^{K}$ and $\{\hat{T}_{d,k'}\}_{k'=1}^{K}$]
v) Match $\hat{f}_{D,k}$ and $\hat{T}_{d,k'}$ based on (23) and (24) for all k, k'.

D. GSD-IC: APPLICATION OF GSD-ST IN FMCW RADAR SYSTEMS

Until now, we have explained how to extract $\{\hat{V}_k, \hat{R}_k\}_{k=1}^{K}$ from $\mathbf{s}$ based on the method of GSD-ST. In this section, we will introduce GSD-IC in an environment where desired and interference signals are mixed. Here, we formulate the received signal model for the presence of interference signal. As shown in Fig. 2, there are three types of received signals:

1) $\mathbf{s}_1(n, m)$: the radar signal transmitted from the ego-vehicle is reflected from the target vehicle and received back to the radar of ego-vehicle.
2) $\mathbf{s}_2(n, m)$: the radar signal transmitted from the ego-vehicle is reflected from the interferer and received back to the radar of ego-vehicle.
3) $\mathbf{s}_3(n, m)$: the radar signal transmitted from the interferer is directly received by the radar of the ego-vehicle.

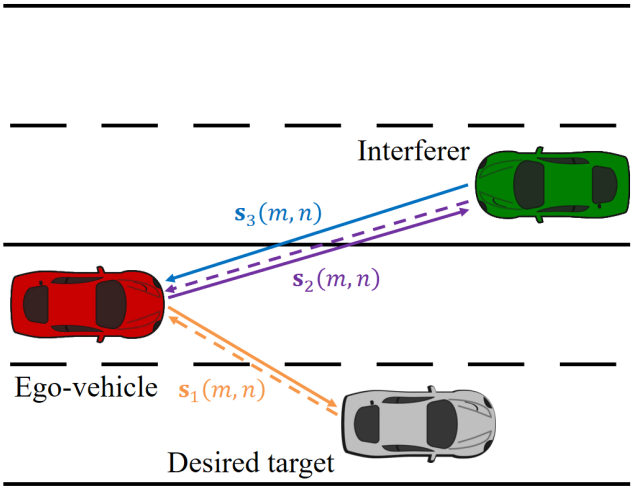

FIGURE 2. An example of the interference situation.

TABLE 1. Parameter settings.

Radar parameter	Value
The number of simulations	3000
Center frequency	76.5 GHz
Operating bandwidth	500 MHz
Sweep time	50 ms
Time-frequency slope	10^{10} s^{-2}
Sampling frequency	13 MHz
Sampling interval	77 ms
Distance to the target	Uniform$(0, 200)$ m
Velocity of the target	Uniform$(0, 20)$ m/s
Distance to the interferer	Uniform$(0, 200)$ m
Velocity of the interferer	Uniform$(-20, 0)$ m/s

Here, an important observation in GSD-IC is that $f_{d,2}$ has the same value for $f_{d,3}$, because both of these parameters are the Doppler frequencies caused by the relative velocity between the ego-vehicle and the interferer. In other words, even if the number of received signals is three, $\mathbf{s}_{:,m}$ for all m consists of two geometric sequences. Based on the Algorithm 1, the functions of $\mathcal{D}_2$ and $\mathcal{R}_2$ are used to estimate the Doppler frequencies and those of $\mathcal{D}_3$ and $\mathcal{R}_3$ are used to estimate the time delays. In addition, we can separate the desired and interference signal by excluding the signals having the almost similar Doppler frequencies. Finally, we can obtain the estimate of velocity and distance of the target, i.e., $\hat{V}_1$ and $\hat{R}_1$, as follows:

$$\hat{V}_1 = \frac{c\hat{f}_{D,1}}{f_c}, \tag{25}$$

and

$$\hat{R}_1 = \frac{c\hat{T}_{d,1}}{2}. \tag{26}$$

IV. PERFORMANCE ANALYSIS

A. SIMULATION SET-UP

In the simulation, we set the values of the parameters as shown in Table 1, which are generally used in automotive radar systems [25]. It is assumed that the ego-vehicle and the interferer use the same FMCW radar system. Therefore, most of the parameters are the same, but only the velocity of the interferer has a negative value because it is assumed that the interference source is running from the opposite lane. For a performance comparison, we select two schemes: the FFT method for peak detection (Baseline 1) [22] and the inverse raised cosine window method (Baseline 2) [26].

B. AN EXAMPLE OF COMPARISON OF DISTANCE AND VELOCITY ESTIMATION RESULTS

Fig. 3 shows an example of the target distance-velocity estimation result. The observed signal, desired target signal, and interference signal are shown in Fig. 3 (a), (b), and (c), respectively. In this experiment, we set the signal-to-interference ratio (SIR) and the signal-to-noise ratio (SNR) to -20 dB and 25 dB, respectively. Fig. 3 (d) shows the estimated distance

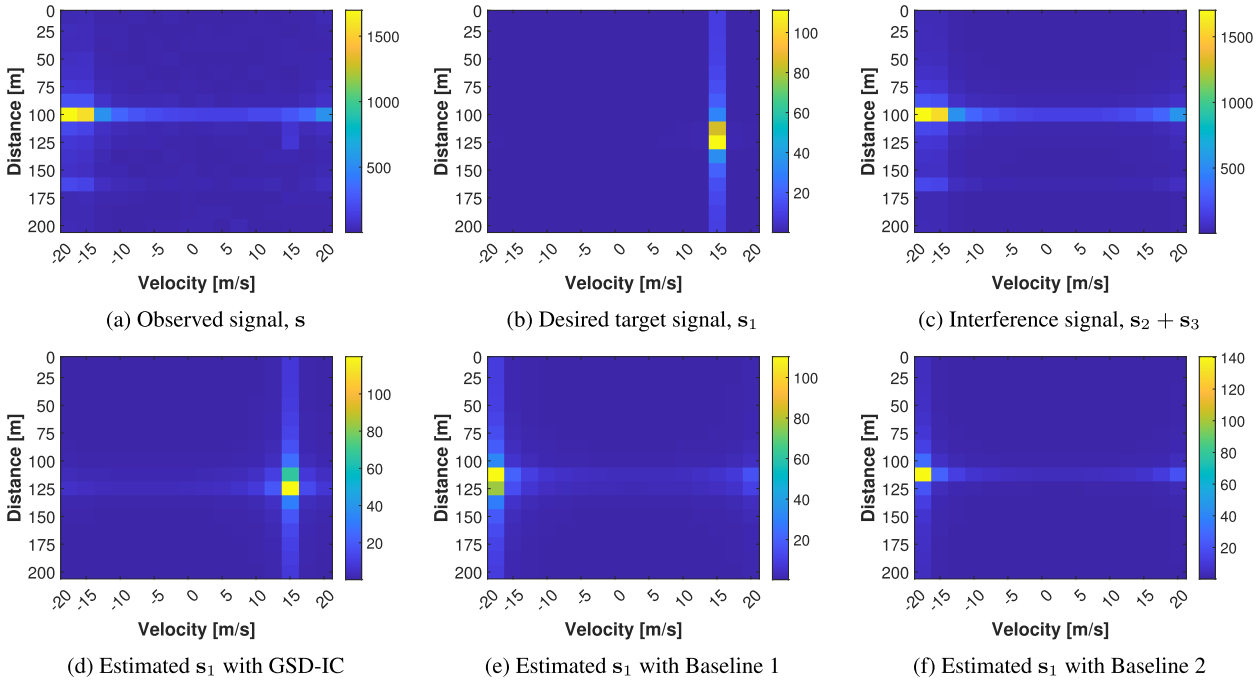

(a) Observed signal, $\mathbf{s}$ (b) Desired target signal, $\mathbf{s}_1$ (c) Interference signal, $\mathbf{s}_2 + \mathbf{s}_3$

(d) Estimated $\mathbf{s}_1$ with GSD-IC (e) Estimated $\mathbf{s}_1$ with Baseline 1 (f) Estimated $\mathbf{s}_1$ with Baseline 2

FIGURE 3. An example of a range-Doppler map (SIR = −20 dB and SNR = 25 dB).

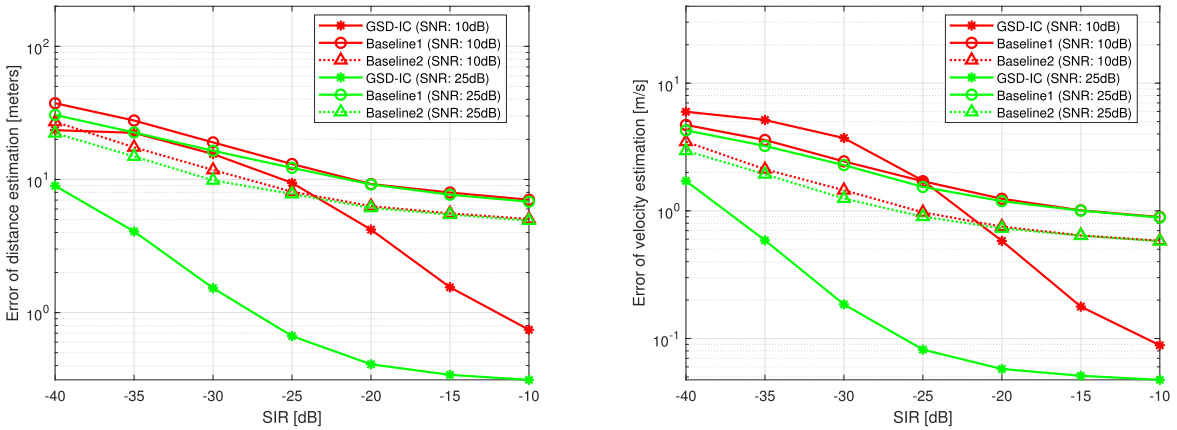

(a) Error of distance estimation (b) Error of velocity estimation

FIGURE 4. Comparison of estimation error according to SIR.

and velocity information of the desired target when the proposed GSD-IC is applied. When comparing the results with Fig. 3 (b), the target information exists at almost the same position in the distance-velocity plane. However, from the detection results of Baselines 1 and 2 (i.e., Figs. 3 (e) and (f)), only information on the distance and velocity of the interferer is extracted. In other words, the target information could not be accurately extracted due to the dominant interference signal in Baselines 1 and 2.

C. ESTIMATION ERROR ACCORDING TO INTERFERENCE LEVEL

First, the errors in the distance and velocity estimation were evaluated, while changing the SIR from −40 to −10 dB. In this simulation, we calculated estimation errors for two different SNR values (i.e., 10 and 25 dB), as shown in Fig. 4. As the SNR increases, the estimation error of the proposed method is significantly smaller than that of the FFT-based estimation method. In addition, even if the SNR becomes higher, the distance and velocity estimation error of the conventional method has not been lowered below a certain level. However, the error of the proposed method converged to zero at high SNR.

D. ESTIMATION ERROR ACCORDING TO NOISE LEVEL

In the next simulation, we evaluated the distance and velocity estimation performance by changing the SNR from −10 to 30 dB, as shown in Fig. 5. In this case, errors in the distance

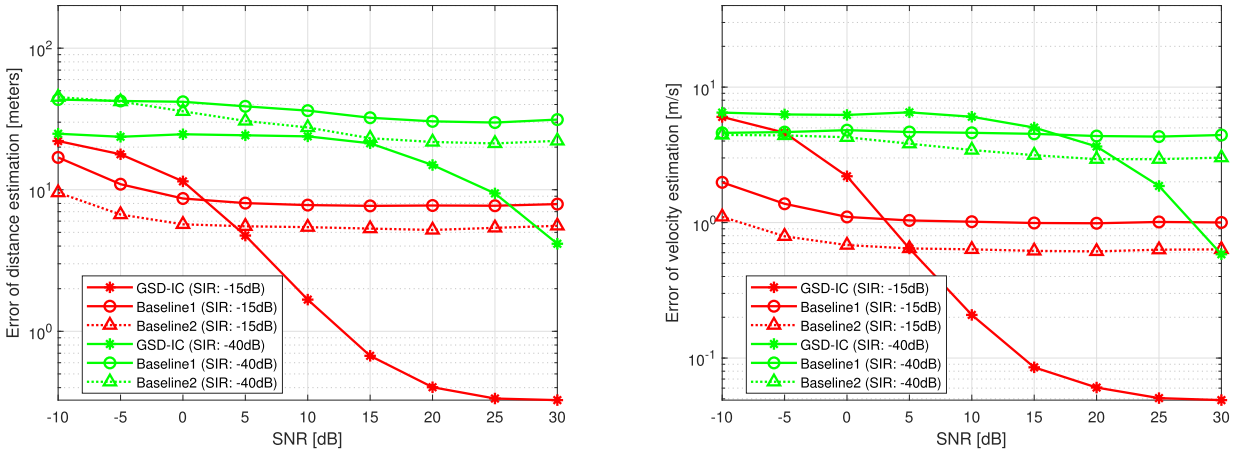

(a) Error of distance estimation

(b) Error of velocity estimation

FIGURE 5. Comparison of estimation error according to SNR.

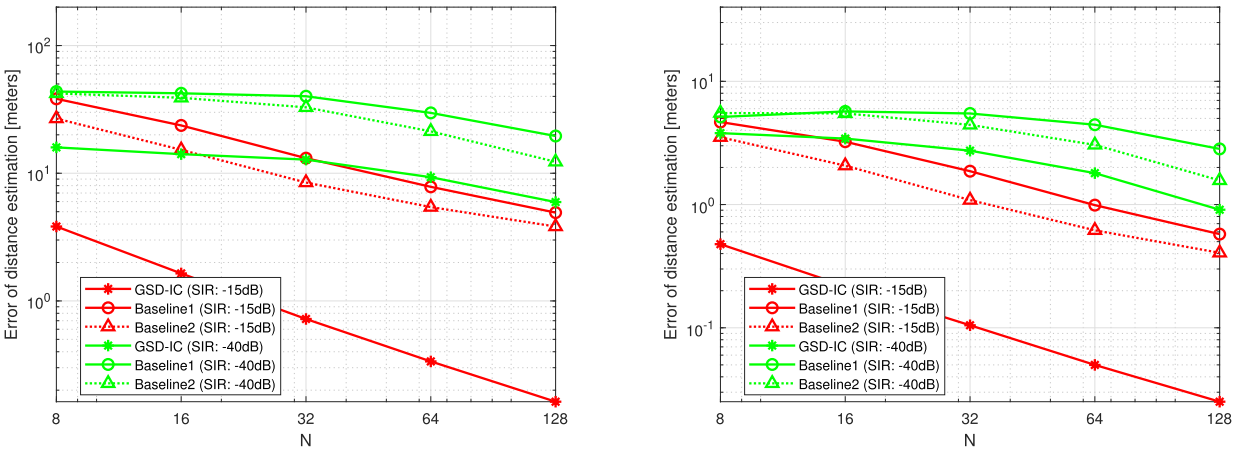

(a) Error of distance estimation

(b) Error of velocity estimation

FIGURE 6. Comparison of estimation error according to N (SNR = 25dB).

and velocity estimation were calculated for two different SIR values: −15 and −40 dB. As the SIR value increases, the performance difference between the FFT-based method and the proposed GSD-IC method becomes more pronounced. In addition, the proposed method shows excellent estimation performance at high SNR values.

E. ESTIMATION ERROR ACCORDING TO THE NUMBER OF 2D SAMPLES

Here, we verified the performance of the proposed method by changing the number of samples N. In this simulation, the SNR value was fixed at 25 dB, and the distance and velocity estimation errors were calculated for the two different SIR values: −15 and −40 dB. Naturally, the estimation accuracy tends to increase when more samples are used for the distance and velocity estimation, which is shown in Fig. 6. In this case as well, when the SIR is high, the performance of the proposed method is clearly distinguished from that of the conventional method.

F. ESTIMATION ERROR ACCORDING TO THE NUMBER OF TARGETS AND INTERFERERS

Finally, we examine the effect of the number of targets and interferers. As shown in Fig. 7, the proposed method shows much lower estimation errors compared to other Baselines for all cases where the SIR is −15 dB or −40 dB. In addition, even if the number of targets increases, GSD-IC estimates the distance and velocity information of the target with low errors than Baseline 1 and 2.

Although GSD-IC generally performs better than other methods, it is sensitive to the increase in the number of interferers. For example, in the SIR −15dB situation in Fig. 8 (b) (in this case, $K = 9$), Baseline 2 shows slightly better performance than our proposed technique. This is because numerical errors may occur when (9) is solved. A closed

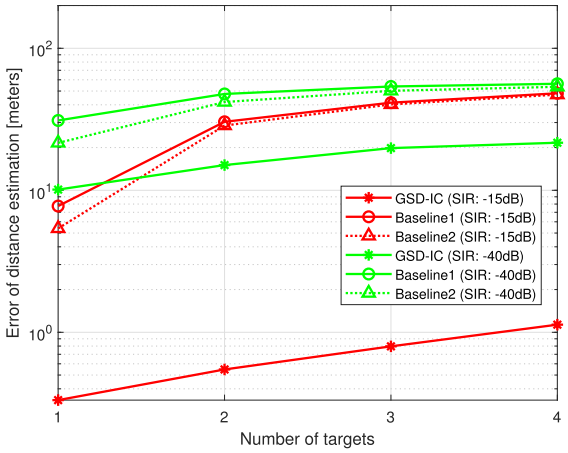

(a) Error of distance estimation

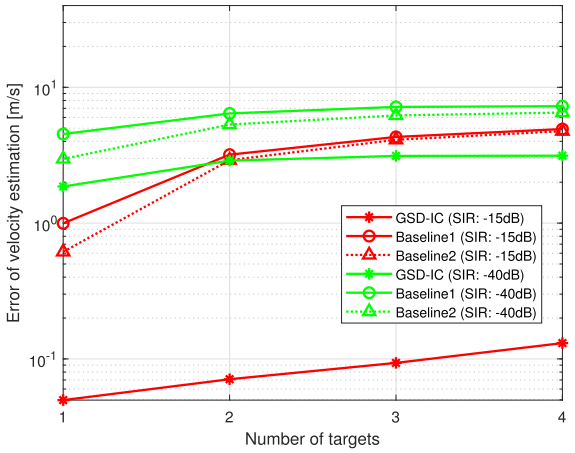

(b) Error of velocity estimation

FIGURE 7. Comparison of estimation error according to the number of targets (SNR = 25dB).

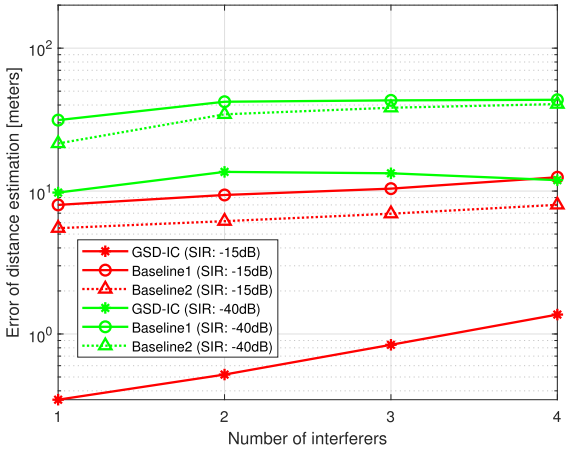

(a) Error of distance estimation

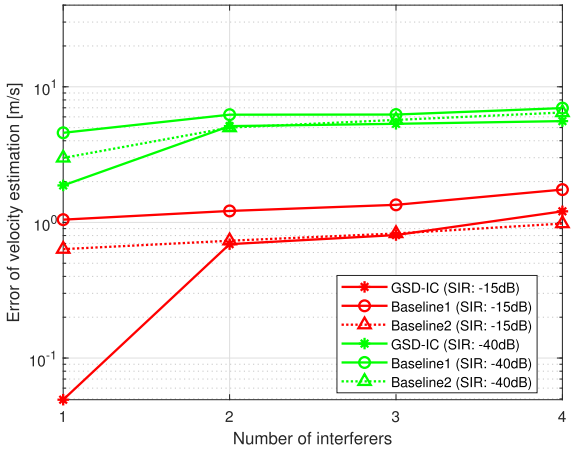

(b) Error of velocity estimation

FIGURE 8. Comparison of estimation error according to the number of interferers (SNR = 25dB).

form solution for (9) exists for lower values of K (such as $K \leq 4$), whereas the performance of supplementary algorithms (such as denoising) play an important role in the accuracy of GSD-IC when $K > 4$.

V. CONCLUSION

In this paper, we proposed a new high-resolution technique for interference cancellation in automotive radar systems, namely GSD-IC method. First, we showed that the geometric sequential representation of the received FMCW signal in 2D samples. Second, we proposed how the delay and Doppler can be jointly estimated based on the geometric sequential analysis in the ideal case and the noisy case. Third, we formulated the mathematical model in which a signal reflected from the desired target a interference signal transmitted from another vehicle's radar were combined. Then, by applying the GSD-IC to the superposed signal, we estimated the amplitude, time delay, and Doppler frequency of each signal. In other words, we could effectively separate the given signal into multiple signals and remove only the interference signal. The proposed GSD-IC method has an advantage that it does not require additional hardware to generate radar waveforms to avoid interference. Furthermore, we believe that the proposed scheme can be extended to the more complex scenarios such as the environments where several vehicles causing interference exist. Combining our developed algorithm with real data also remains an important further research.

REFERENCES

[1] M. Khader and S. Cherian. An introduction to automotive LiDAR. Texas Instruments, Dallas, TX, USA. Accessed: Apr. 1, 2021. [Online]. Available: https://www.ti.com/lit/wp/slyy150a/slyy150a.pdf
[2] M. Schneider, "Automotive radar-status and trends," in *Proc. German Microw. Conf. (GeMiC)*, Ulm, Germany, Apr. 2005, pp. 144–147.
[3] S. Lee, Y.-J. Yoon, J.-E. Lee, and S.-C. Kim, "Human-vehicle classification using feature-based SVM in 77-GHz automotive FMCW radar," *IET Radar, Sonar Navigat.*, vol. 11, no. 10, pp. 1589–1596, Oct. 2017.

[4] A. Angelov, A. Robertson, R. Murray-Smith, and F. Fioranelli, "Practical classification of different moving targets using automotive radar and deep neural networks," *IET Radar, Sonar Navigat.*, vol. 12, no. 10, pp. 1082–1089, Oct. 2018.
[5] J.-E. Lee, H.-S. Lim, S.-H. Jeong, S.-C. Kim, and H.-C. Shin, "Enhanced iron-tunnel recognition for automotive radars," *IEEE Trans. Veh. Technol.*, vol. 65, no. 6, pp. 4412–4418, Jun. 2016.
[6] H. Sim, T.-D. Do, S. Lee, Y.-H. Kim, and S.-C. Kim, "Road environment recognition for automotive FMCW RADAR systems through convolutional neural network," *IEEE Access*, vol. 8, pp. 141648–141656, 2020.
[7] T.-N. Luo, C.-H. E. Wu, and Y.-J. E. Chen, "A 77-GHz CMOS automotive radar transceiver with anti-interference function," *IEEE Trans. Circuits Syst. I, Reg. Papers*, vol. 60, no. 12, pp. 3247–3255, Dec. 2013.
[8] M. Goppelt, H.-L. Blöcher, and W. Menzel, "Automotive radar-investigation of mutual interference mechanisms," *Adv. Radio Sci.*, vol. 8, pp. 55–60, Sep. 2010.
[9] G. M. Brooker, "Mutual interference of millimeter-wave radar systems," *IEEE Trans. Electromagn. Compat.*, vol. 49, no. 1, pp. 170–181, Feb. 2007.
[10] S. Heuel, "Automotive radar interference test," in *Proc. 18th Int. Radar Symp. (IRS)*, Prague, Czech Republic, Jun. 2017, pp. 1–7.
[11] L. Mu, T. Xiangqian, S. Ming, and Y. Jun, "Research on key technologies for collision avoidance automotive radar," in *Proc. IEEE Intell. Vehicles Symp.*, Xi'an, China, Jun. 2009, pp. 233–236.
[12] T.-H. Liu, M.-L. Hsu, and Z.-M. Tsai, "Mutual interference of pseudorandom noise radar in automotive collision avoidance application at 24 GHz," in *Proc. IEEE 5th Global Conf. Consum. Electron.*, Kyoto, Japan, Oct. 2016, pp. 1–2.
[13] Z. Xu and Q. Shi, "Interference mitigation for automotive radar using orthogonal noise waveforms," *IEEE Geosci. Remote Sens. Lett.*, vol. 15, no. 1, pp. 137–141, Jan. 2018.
[14] J. Bechter, C. Sippel, and C. Waldschmidt, "Bats-inspired frequency hopping for mitigation of interference between automotive radars," in *IEEE MTT-S Int. Microw. Symp. Dig.*, San Diego, CA, USA, May 2016, pp. 1–4.
[15] X. Yang, K. Zhang, T. Wang, and Y. Zhao, "Anti-interference waveform design for automotive radar," in *Proc. IEEE 2nd Adv. Inf. Technol., Electron. Autom. Control Conf. (IAEAC)*, Chongqing, China, Mar. 2017, pp. 14–17.
[16] M. A. Hossain, I. Elshafiey, and A. Al-Sanie, "Mutual interference mitigation in automotive radars under realistic road environments," in *Proc. 8th Int. Conf. Inf. Technol. (ICIT)*, Amman, Jordan, May 2017, pp. 895–900.
[17] J. Bechter and C. Waldschmidt, "Automotive radar interference mitigation by reconstruction and cancellation of interference component," in *IEEE MTT-S Int. Microw. Symp. Dig.*, Heidelberg, Germany, Apr. 2015, pp. 1–4.
[18] J. Bechter, K. D. Biswas, and C. Waldschmidt, "Estimation and cancellation of interferences in automotive radar signals," in *Proc. 18th Int. Radar Symp. (IRS)*, Prague, Czech Republic, Jun. 2017, pp. 1–10.
[19] J.-H. Choi, H.-B. Lee, J.-W. Choi, and S.-C. Kim, "Mutual interference suppression using clipping and weighted-envelope normalization for automotive FMCW radar systems," *IEICE Trans. Commun.*, vol. E99-B, no. 1, pp. 280–287, Jan. 2016.
[20] S. Lee, J. Lee, and S. Kim, "Mutual interference suppression using wavelet denoising in automotive FMCW radar systems," *IEEE Trans. Intell. Transp. Syst.*, vol. 22, no. 2, pp. 887–897, Feb. 2021.
[21] F. Uysal, "Synchronous and asynchronous radar interference mitigation," *IEEE Access*, vol. 7, pp. 5846–5852, 2018.
[22] S. M. Patole, M. Torlak, D. Wang, and M. Ali, "Automotive radars: A review of signal processing techniques," *IEEE Signal Process. Mag.*, vol. 34, no. 2, pp. 22–35, Mar. 2017.
[23] W.-H. Lee, J.-H. Lee, and K. W. Sung, "Geometric sequence decomposition with k-simplexes transform," *IEEE Trans. Commun.*, vol. 69, no. 1, pp. 94–107, Jan. 2021.
[24] A. V. Aho, J. E. Hopcroft, and J. D. Ullman, *The Design and Analysis of Computer Algorithms*. Reading, MA, USA: Addison-Wesley, 1974.
[25] J. Hatch, A. Topak, R. Schnabel, T. Zwick, R. Weigel, and C. Waldschmidt, "Millimeter-wave technology for automotive radar sensors in the 77 GHz frequency band," *IEEE Trans. Microw. Theory Techn.*, vol. 60, no. 3, pp. 845–860, Mar. 2012.
[26] M. Barjenbruch, D. Kellner, K. Dietmayer, J. Klappstein, and J. Dickmann, "A method for interference cancellation in automotive radar," in *IEEE MTT-S Int. Microw. Symp. Dig.*, Heidelberg, Germany, Apr. 2015, pp. 1–4.

WOONG-HEE LEE (Member, IEEE) received the B.S. degree in electrical engineering from the Korea Advanced Institute of Science and Technology (KAIST), Daejeon, South Korea, in 2009, and the Ph.D. degree in electrical engineering from Seoul National University, Seoul, South Korea, in 2017. From 2017 to 2019, he was an Experienced Researcher with the Advanced Standard Research and Development Laboratories, LG Electronics Inc., Seoul. From 2019 to 2020, he was a Postdoctoral Researcher with the Department of Communication Systems, KTH Royal Institute of Technology, Stockholm, Sweden. He was an Experienced Researcher with Ericsson Research, Stockholm. Since March 2021, he has been an Assistant Professor with the Department of Control and Instrumentation Engineering, Korea University, Sejong-si, Republic of Korea. His research interests include signal processing, machine learning, and game theory in wireless communications.

SEONGWOOK LEE (Member, IEEE) received the B.S. and Ph.D. degrees in electrical and computer engineering from Seoul National University (SNU), Seoul, Republic of Korea, in February 2013 and August 2018, respectively. From September 2018 to February 2020, he worked as a Staff Researcher with the Machine Learning Laboratory, AI & SW Research Center, Samsung Advanced Institute of Technology (SAIT), Gyeonggi-do, Republic of Korea. Since March 2020, he has been an Assistant Professor with the School of Electronics and Information Engineering, College of Engineering, Korea Aerospace University (KAU), Gyeonggi-do. His research interests include radar signal processing techniques, such as enhanced target detection and tracking, target recognition and classification, clutter suppression and mutual interference mitigation, and multiple-input and multiple-output radar imaging. He received the Distinguished Ph.D. Dissertation Award from the Department of Electrical and Computer Engineering, SNU, and published more than 70 papers on radar signal processing.